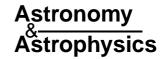
A&A 457, 721-728 (2006)

DOI: 10.1051/0004-6361:20065324

© ESO 2006



### Atomic data from the Iron Project\*

# LXII. Allowed and forbidden transitions in Fe XVIII in relativistic Breit-Pauli approximation

S. N. Nahar

Department of Astronomy, The Ohio State University, Columbus, OH 43210, USA

e-mail: nahar@astronomy.ohio-state.edu

Received 30 March 2006 / Accepted 4 July 2006

#### **ABSTRACT**

An extensive set of oscillator strengths (f), line strengths (S) and radiative decay rates (A) for the allowed and forbidden transitions in Fe XVIII is presented. The results include 1174 fine structure levels of total angular momenta J=1/2-17/2 of even and odd parities with  $2 \le n \le 10$ ,  $0 \le l \le 9$ , orbital angular momenta,  $0 \le L \le 11$ , and spin multiplicities 2, 4. These yeild about 171 500 transitions. The allowed electric dipole (E1) transitions, 141 869 in total, are obtained in the close coupling approximation using the relativistic Breit-Pauli R-matrix (BPRM) method. The forbidden electric quadrupole (E2), octupole (E3), and magnetic dipole (M1), quadrupole (M2) transitions, 29 682 in total, are obtained from configuration interaction Breit-Pauli atomic structure calculations using the code SUPERSTRUCTURE. The close coupling wavefunction expansion for Fe XVIII includes 10 levels of configurations  $2s^22p^4$ ,  $2s2p^5$ , and  $2p^6$  in the BRPM calculations. All fine structure levels have been identified spectroscopically. Comparison of the present energies with the available observed energies shows very good agreement. The lifetime of level  $2s2p^6$  S calculated from the present radiative decay rate agrees very well with the single measurement. The present decay rate for the well known E2 line arising from  $2p^5(^2P_{3/2}^{\circ} - ^2P_{1/2}^{\circ})$  transition within the ground state term also agrees almost exactly with NIST tabulated value. However, varying degree of agreement is found with previously calculated values for some transitions.

Key words. atomic processes – atomic data – line: formation – X-rays: general – ultraviolet: general – infrared: general

#### 1. Introduction

Highly charged iron ions exist in a variety of high-temperature astrophysical sources emiting or absorbing radiation in the range from the optical to the X-ray. The spectral lines of these ions provide information about physical conditions and chemical abundances in the sources. The analysis and modeling of these spectra require accurate radiative data. The present report provides the atomic data for flourine like ion Fe XVIII obtained in the first ab initio calculations using the relativistic Breit-Pauli approximation under the Iron Project (IP, Hummer et al. 1993), a program for systematic study of iron and iron-group atoms and ions (e.g. Fe V by Nahar et al. 2000; Fe XVII by Nahar et al. 2003; Fe XX by Nahar 2003; Fe XXI by Nahar, Fe XXIV and Fe XXV by Nahar & Pradhan 1999).

Limited and inadequate amount of atomic data are available for Fe XVIII and mainly for the low-lying transitions. For example, the web based compiled database of the National Institute for Standards and Technology (NIST) contains 66 observed levels and 83 transitions for Fe XVIII from several investigators. However, many more lines of low and high excitation/ionization of most ionized stages of iron are found in observations from space based UV and X-ray observatories such as the HST, FUSE, Chandra and XMM-Newton. Hence, the present consideration of a large number of transitions should meet most of the practical needs for the atomic transitions in Fe XVIII.

#### 2. Theory

The calculations are carried out in the relativistic Breit-Pauli approximation using two different approaches. The electric dipole allowed (E1) transitions are obtained in the close coupling (CC) approximation using the Breit-Pauli R-matrix (BPRM) method developed under the Iron Project (IP, Hummer et al. 1993; Scott & Burke 1980; Scott & Taylor 1982; Berrington et al. 1987, 1995). The forbidden electric quadrupole (E2), octupole (E3), and magnetic dipole (M1), quadrupole (M2) transitions are obtained from configuration interaction atomic structure calculations using the latest version of the SUPERSTRUCTURE (Eissner et al. 1974; Eissner & Zeippen 1981; Eissner 1991; Nahar et al. 2003).

The BPRM method enables calculation of both the dipole allowed (no change in spin, i.e.,  $\Delta S=0$ ) and the intercombination ( $\Delta S\neq 0$ ) E1 transition probabilities in intermediate coupling, and yields a large number of fine structure transition probabilities with high accuracy. The theoretical details of the relativistic BPRM method are discussed in previous works, such as in the first large scale relativistic BPRM calculations for bound-bound transitions in Fe XXIV and Fe XXV (Nahar & Pradhan 1999) and subsequent papers (e.g. Nahar & Pradhan 2000; Nahar et al. 2000, 2003). A detailed description of atomic structure calculations for the forbidden transitions, involving the various terms in the Breit-Pauli Hamiltonian, are presented in Nahar et al. (2003) and Nahar (2003). Below, a brief outline of the calculations using both the approaches is presented.

<sup>\*</sup> Full Tables 3a, 3b, 4, 5, 7 and 8 are only available at the CDS via anonymous ftp to cdsarc.u-strasbg.fr (130.79.128.5) or via http://cdsweb.u-strasbg.fr/cgi-bin/qcat?J/A+A/457/721

In the CC approximation the wavefunction expansion,  $\Psi_E$ , for a (N+1) electron system with total orbital angular momentum L, spin multiplicity (2S+1), and total angular momentum symmetry  $J\pi$ , is written in terms of the states of the N-electron target ion as

$$\Psi_{\rm E}({\rm e+ion}) = A \sum_i \chi_i({\rm ion})\theta_i + \sum_j c_j \Phi_j({\rm e+ion}), \tag{1}$$

where  $\chi_i$  is the target ion wavefunction in a specific state  $S_i L_i \pi_i$  or level  $J_i \pi_i$ , and  $\theta_i$  is the wavefunction for the interacting (N+1)th electron in a channel labeled as  $S_i L_i (J_i) \pi_i \ k_i^2 \ell_i (S L \pi \ or \ J \pi)$  where  $k_i^2$  is the incident kinetic energy.  $\Phi_j$ 's are correlation wavefunctions of the (N+1) electron system that (a) compensate for the orthogonality conditions between the continuum and the bound orbitals and (b) represent additional short-range correlation that is often of crucial importance in scattering and radiative CC calculations for each  $S L \pi$ .

The relativistic Hamiltonian for the system of *N*-electron target ion and a free/bound electron in the Breit-Pauli approximation is

$$H_{N+1}^{\text{BP}} = H_{N+1} + H_{N+1}^{\text{mass}} + H_{N+1}^{\text{Dar}} + H_{N+1}^{\text{so}} + \frac{1}{2} \sum_{i \neq j}^{N} [g_{ij}(so + so') + g_{ij}(ss') + g_{ij}(css') + g_{ij}(d) + g_{ij}(oo')], \quad (2)$$

where  $H_{N+1}$  is the non-relativistic Hamiltonian,

$$H_{N+1} = \sum_{i=1}^{N+1} \left\{ -\nabla_i^2 - \frac{2Z}{r_i} + \sum_{j>i}^{N+1} \frac{2}{r_{ij}} \right\}$$
 (3)

 $H_{N+1}^{\rm mass}$  is the mass correction,  $H_{N+1}^{\rm Dar}$  is the Darwin, and  $H_{N+1}^{\rm so}$  is the spin-orbit interaction term respectively. The two-body interaction terms are with notation c for contraction, d for Darwin, o for orbit, s for spin and a prime indicates "other". All terms improve the energies except the spin-orbit interaction term which splits the energies into fine structure components. The BPRM Hamiltonian under the IP ignores the two-body spin-spin and spin-other-orbit terms for the relatively stronger E1 transitions. However, the atomic structure calculations for the forbidden transitions include the contribution of the full Breit interaction term consisting of the fine structure terms, that is spin-other-orbit (os') and spin-other-spin (ss') terms and ignores the last three two-body interaction terms.

In the BPRM method, the set of  $SL\pi$  are recoupled to obtain (e + ion) states with total  $J\pi$ , following the diagonalization of the (N+1)-electron Hamiltonian,

$$H_{N+1}^{BP}\Psi = E\Psi. (4)$$

Substitution of the wavefunction expansion introduces a set of coupled equations that are solved using the R-matrix approach. At negative total energies (E < 0), the solutions of the close coupling equations occur at discrete eigenvalues of the (e + ion) Hamiltonian that correspond to pure bound states  $\Psi_B$ .

For the E1 transitions, the oscillator strength (f) is proportional to the generalized line strength, in length form, as

$$S = \left| \left\langle \Psi_{\rm f} \middle| \sum_{j=1}^{N+1} r_j \middle| \Psi_{\rm i} \right\rangle \right|^2 \tag{5}$$

where  $\Psi_i$  and  $\Psi_f$  are the initial and final bound wave functions respectively. The line strengths are energy independent quantities. This gives the oscillator strength,

$$f_{ij} = \frac{E_{ji}}{3g_i}S,\tag{6}$$

and the radiative decay rate or Einstein's A-coefficient

$$A_{ji}(au) = \frac{1}{2}\alpha^3 \frac{g_i}{g_i} E_{ji}^2 f_{ij}.$$
 (7)

 $E_{ji}$  is the energy difference between the initial and final states,  $\alpha$  is the fine structure constant, and  $g_i$ ,  $g_j$  are the statistical weight factors of the initial and final states, respectively.

The transition rates for excitation or de-excitation via various types of forbidden transitions can be obtained from the general line strength,

$$S^{X\lambda}(ij) = \left| \left\langle \Psi_j \middle\| O^{X\lambda} \middle\| \Psi_i \right\rangle \right|^2, \qquad S(ji) = S(ij), \tag{8}$$

where X represents the electric or magnetic type and  $\lambda$  represents various multipoles, such as dipole (1), quadrupole (2), octupole (3) (e.g., Nahar et al. 2003). Hence, the oscillator strength,  $f_{ij}$ , and the radiative decay rates for electric dipole (E1) transition above can be obtained from line strength,  $S^{E1}$ . The A-values for spontaneous decays by higher order multipole radiation are as follows:

electric quadrupole (E2) and magnetic dipole (M1)

$$g_j A_{ji}^{E2} = 2.6733 \times 10^3 \text{ s}^{-1} (E_j - E_i)^5 S^{E2}(i, j)$$
 (9)

$$g_i A_{ii}^{M1} = 3.5644 \times 10^4 \text{ s}^{-1} (E_i - E_i)^3 S^{M1}(i, j);$$
 (10)

and for electric octopole (E3) and magnetic quadrupole (M2)

$$g_j A_{ji}^{E3} = 1.2050 \times 10^{-3} \text{ s}^{-1} (E_j - E_i)^7 S^{E3}(i, j)$$
 (11)

$$g_j A_{ji}^{M2} = 2.3727 \times 10^{-2} \text{ s}^{-1} (E_j - E_i)^5 S^{M2}(i, j).$$
 (12)

The lifetime of a level can be obtained from the A-values as,

$$\tau_k(s) = \frac{1}{\sum_i A_{ki}(s^{-1})},\tag{13}$$

where the sum is the total radiative transition probability for the level k, and  $A_{ji}(s^{-1}) = A_{ji}(au)/\tau_0$ ,  $\tau_0 = 2.4191 \times 10^{-17}$  s is the atomic unit of time.

#### 3. Calculations

#### 3.1. BPRM calculations for E1 transitions

The CC calculations using the BPRM method proceed in several stages. A brief description is given below for the computations of *A*-values for E1 transitions in Fe XVIII.

The initial step of the calculation is to construct an accurate representation of the target or core ion eigenstates. The wavefunction expansion for the Fe XVIII consists of 10 fine strucuture levels (Table 1) of configurations 2s<sup>2</sup>2p<sup>4</sup>, 2s2p<sup>5</sup>, 2p<sup>6</sup> of the target Fe XIX. The target wavefuctions were obtained from atomic structure calculations using SUPERSTRUCTURE (Eissner et al. 1974). The actual wavefunction correspond to a much larger set of spectroscopic configurations, thirteen in total given in Table 1, with orbitals going upto 4d. However, a smaller set of 10 levels is chosen for the present calculation since no bound states are expected to form with core excitation beyond these lowest levels. Table 1 lists the values of Thomas-Fermi scaling parameters for individual orbitals  $\lambda_{nl}$  employed in the atomic structure calculations and the energies of the levels. The  $\lambda_{nl}$  paramters are obtained through optimization of the energies and oscillator strengths of the target. It was found that inclusion of proper configurations are more sensitive to optimization of the wavefunction than the changes in  $\lambda_{nl}$  values.

**Table 1.** Fine strucuture levels and relative energies ( $E_t$ ) of the target (core) ion Fe XIX in the wavefunction expansion of Fe XVIII. The atomic structure calculations for Fe XIX employs the set of spectroscopic configurations:  $2s^22p^4$ ,  $2s2p^5$ ,  $2p^6$ ,  $2s^22p^33s$ ,  $2s^22p^33p$ ,  $2s^22p^34s$ ,  $2s^22p^34p$ ,  $2s^22p^34d$ ,  $2s2p^43s$ ,  $2s2p^43p$ ,  $2s2p^43d$ ,  $2s^22p^23s^2$ , and the Thomas-Fermi scaling parameters for the orbitals:  $\lambda_{nl} = 1.35(1s)$ , 1.25(2s), 1.12(2p), 1.07(3s), 1.05(3p), 1.10(3d), 1.0(4s), 1.0(4p), 1.0(4d). The notation "Obs" is for observed and "Cal" for calculated energies.

_				
	Term	$J_{t}$	$E_{\rm t}({\rm Ry})$	$E_{\rm t}({\rm Ry})$
			Obs	Cal
1	$2s^22p^4(^3P)$	2	0.0	0.
2	$2s^22p^4(^3P)$	0	0.685	0.678542
3	$2s^22p^4(^3P)$	1	0.81505	0.822163
4	$2s^22p^4(^1D)$	2	1.53869	1.590916
5	$2s^22p^4(^1S)$	0	2.9628	3.000582
6	$2s2p^5(^3P^\circ)$	2	8.4099	8.517784
7	$2s2p^{5}(^{3}P^{\circ})$	1	8.9736	9.099065
8	$2s2p^5(^3P^\circ)$	0	9.38623	9.517837
9	$2s2p^{5}(^{1}P^{\circ})$	1	11.551	11.792658
10	$2p^{6}(^{1}S)$	0	19.4480	19.941113

The relative observed energies in Table 1 are available in the NIST compiled database. Good agreement can be seen between the calculated and observed energies. However, the observed energies are used in the BPRM calculations for improved accuracy. The A-values of Fe XIX transitions for the set considered also compare well with those in the NIST table. For example, for the first allowed transition,  $2s^22p^4(^3P_2) - 2s2p^5(^3P_2^\circ)$ present A-value is  $3.62e+10 \text{ s}^{-1}$  compared to  $3.9e+10 \text{ s}^{-1}$ , for the  $2s^22p^4(^3P_2)-2s2p^5(^3P_1^\circ)$  transition is  $2.99e+10 s^{-1}$  compared to  $3.17e+10 \text{ s}^{-1}$  in the NIST table. The f-values show varying degrees of agreement from good to poor between the length and velocity forms. Inclusion of more configurations improves wavefunction in the near region than the aymptotic region resulting in more accurate f-values in the length form and a difference in the length and velocity forms. The thirteen configurations specified in Table 1 for Fe XIX were treated as spectroscopic in the atomic structure calculations. Hence a large set of energies and transitions (allowed and forbidden) have been obtained for this ion. They will be published in a separate paper with more comparisons with others.

The bound-channel term of the wavefunction, the second term in Eq. (1), includes 96 possible (N + 1)-configurations from vacant orbitals to maximum occupancies  $2s^2$ ,  $2p^6$ ,  $3s^2$ ,  $3d^2$ ,  $4s^2$ ,  $4p^2$ , 4d and from  $3p^2$  to  $3p^6$ .

The BPRM packages of codes (Berrington et al. 1995) begin with the orbital wavefunctions of the target or the core eigenstates. STG1 computes the one- and two-electron radial integrals. The (e + ion) algebraic and angular coefficients are computed in STG2. The intermediate coupling calculations are enabled on recoupling the LS symmetries in a pair-coupling representation in stage RECUPD. The (e + core) Hamiltonian matrix is diagonalized for each resulting  $J\pi$  in STGH.

Calculations for Fe XVIII transitions included all possible bound levels for  $1/2 \le J \le 17/2$  of even and odd parities, with  $n \le 10$ ,  $l \le 9$ ,  $0 \le L \le 11$ , and spin multiplicities, (2S + 1) = 2, 4. The fine structure bound levels are obtained on scanning through the poles in the (e + ion) Hamiltonian with a fine mesh of effective quantum number  $\nu$ , at  $\Delta \nu = 0.001$  or less in STGB. This requires orders of magnitude more CPU time and memory compared to that for LS coupling calculations. Since the fine structure components lie in small energy gaps, a very fine mesh

is often essential to avoid any missing levels and to obtain accurate energies for high-lying levels.

The theoretical fine structure energy levels have been identified spectroscopically by analysing quantum defects, possible matching components of the relevant LS terms, and channel percentage contributions corresponding to the integrated wavefunctions in the outer region. Although these criteria are built into the identification code PRCBPID (Nahar & Pradhan 2000), it can assign only possible identifications which are then sorted out manually using the following procedure for final identification. Each level is assigned with one or more LS terms based on its dominant channel which provides the information on the configuration, LS term and J value of the core and outer or the valence electron. The levels yield quantum defects relative to the parent target level  $S_iL_iJ_i$  to which a given Rydberg series of bound levels  $(S_iL_iJ_i)n\ell$  belongs. The identification of the low lying levels are reconfirmed by comparing with those of available levels, especially those found in the NIST database. Hund's rule is also followed for levels from the same configurations in that the level with higher angular orbital momentum L and/or higher spin multiplicity will lie lower than those with lower L and lower spin. The final designation is assigned as  $C_t(S_tL_t\pi_t)J_tnlJ(SL)\pi$ , where  $C_t$ ,  $S_t L_t \pi_t$ ,  $J_t$  are the configuration, LS term, parity, and total angular momentum of the target, nl are the principal and orbital quantum numbers of the outer or the valence electron, and J and  $SL\pi$  are the total angular momentum, LS term and parity of the (N+1)-electron system. In addition the level identification procedure establishes a unique correspondence between the fine structure levels and their LS terms such that exact number of fine structure levels are accounted for each LS term.

The bound-bound transitions are computed using STGBB. All transitions have been processed for proper energies and transition wavelengths using code PBPRAD. The calculated energies have been replaced by the available measured energies for improved accuracy. A set of transitions employing only the observed set of levels has been processed with complete spectroscopic notation for direct comparison with experiment and other, such as for diagnostic applications.

## 3.2. Atomic structure calculations for the forbidden transitions

The calculations for forbidden transitions in Fe XVIII include 15 configurations with orbitals going up to 4f. They are listed in Table 7. The  $\lambda_{nl}$  parameters for the orbitals are 1.35(1s), 1.25(2s), 1.15(2p), 1.2(3s), 1.15(3p), 1.1(3d), 1.0(4s), 1.0(4p), 1.0(4d), 1.0(4f). All fifteen configurations included in the atomic structure calculations are treated as spectroscopic. These configurations yeild 108 LS terms and 243 fine structure levels. As mentioned earlier the configuration interaction atomic structure calculations were carried out using the code SUPERSTUCTURE. However, it is the later version of the code that was used for higher multipole transitions in Fe XVII (Nahar et al. 2003) for the first time. Present computations include electric octupole (E3) and magnetic quadrupole (M2) transitions in addition to electric dipole (E1), quadrupole (E2), and magnetic dipole (M1) transitions in Breit-Pauli approximation. All transitions among the 243 fine structure levels are considered. The transitions have been processed by replacing the calculated energies by the limited number of observed energies using the code PRCSS.

#### 4. Results and discussion

The atomic parameters for oscillator strengths (f-values), line strengths (S), and radiative decay rates (A-values) for E1 (dipole allowed and intercombination), and forbidden electric quadrupole (E2), octupole (E3), magnetic dipole (M1) and quadrupole (M2) fine structure transitions in flourine-like Fe XVIII are presented. The large set of atomic data for various transitions should comprise a reasonably complete set for all practical applications for this ion.

The results on the energy levels, oscillator strengths for E1 transitions, and radiative decay rates for forbidden E2, E3, M1, M2 transitions are discussed separately below.

#### 4.1. Theoretical energy levels

A total of 1174 bound fine structure levels are obtained theoretically for Fe XVIII. They correspond to total angular momenta  $1/2 \le J \le 17/2$  of even and odd parities with  $n \le 10$ ,  $0 \le l \le 9$ , total orbital angular momenta  $0 \le L \le 12$  and spin multiplicities 2, 4.

In Table 2 the present energies are compared with the available observed energy levels compiled by NIST. Sixty six levels are listed in the compiled table where 47 levels have proper spectroscopic identification. Each of these levels has been identified in the present set of energy levels. Comparison between the present calculated BPRM energies and the measured values in Table 2 shows that most of the calculated levels are well within 1% of the measured energies, with the largest discrepancy being 3% for the level  $2s^22p^4(^1D)6d(^2D_{3/2})$ . The level index,  $I_J$ , in the table, is the position of the calculated level in the given  $J\pi$  symmetry. The index establishes the correspondence between the calculated and the observed levels.

Spectroscopic identification of the large number of calculated energy levels are assigned with the most possible designation based on the criteria as described in the computation section. The present BPRM approach provides information of percent contributions of various channels to an energy level only from the outer region of the R-matrix boundary. Hence some uncertainty exists in the most dominating channel and to spectroscopic identification, especially for the mixed states.

The complete set of calculated energy levels of Fe XVIII is available eletronically. Following previous works, (e.g. Nahar et al. 2000) the energies are presented in two formats for various practical purposes: (i) in LSJ component format where fine structure levels are grouped as components of a LS term showing spectroscopically completeness of the set, and (ii) in  $J\pi$  set where levels of the symmetry are listed in ascending order of energy positions, as described below.

#### 4.1.1. LSJ term format

In this format the fine structure levels *LSJ* are grouped together according to the same configuration *CLSJ*, useful for spectroscopic diagnostics. It provides the check for completeness of the set of energy levels that belong to the *LS* term, and detects any missing level.

Table 3a presents a sample set of Fe XVIII levels in this format. Various columns provide the core information,  $C_t(SL\pi J)_t$ , the configuration of the outer electron, nl, total angular momentun, J, energy in Rydbergs, the effective quantum number of the valence electron,  $v = \frac{1}{\sqrt{E} - E_t}$ , where  $E_t$  is the next immediate target threshold energy, and the possible LS term designations of the level. No effective quantum number is assigned for

**Table 2.** Comparison of calculated BPRM absolute energies,  $E_{\rm c}$ , of Fe XVIII with observed values,  $E_{\rm o}$ , compiled by NIST.  $I_J$  is the level index for the calculated energy position in symmetry  $J\pi$ . The asterisk next to a J-value indicates that the term has missing fine structure components in the observed set.

Level		J	$I_J$	$E_{\rm o}({\rm Ry})$	$E_{\rm c}({\rm Ry})$
$2s^22p^5$	$^{2}\mathbf{P}^{\circ}$	1.5	1	9.98766E+01	1.00100E+02
$2s^22p^5$	$^{2}\mathbf{P}^{\circ}$	0.5	1	9.89033E+01	9.91652E+01
$2s^2p^6$	$^{2}S$	0.5	1	9.00804E+01	9.03977E+01
$2s^22p^4(3P)3s$	$^{4}P$	2.5	1	4.30800E+01	4.34010E+01
$2s^22p^4(3P)3s$	$^{4}P$	1.5	1	4.28328E+01	4.25270E+01
$2s^22p^4(3P)3s$	$^4P$	0.5	2	4.23643E+01	4.25972E+01
$2s^22p^4(3P)3s$	$^{2}\mathbf{P}$	1.5	2	4.21900E+01	4.31631E+01
$2s^22p^4(3P)3s$	$^{2}\mathbf{P}$	0.5	3	4.19622E+01	4.23020E+01
$2s^22p^4(1D)3s$	$^{2}D$	2.5	2	4.14001E+01	4.17789E+01
$2s^22p^4(1D)3s$	$^{2}D$	1.5	3	4.13657E+01	4.17443E+01
$2s^22p^4(1S)3s$	$^{2}S$	0.5	4	3.99696E+01	4.01833E+01
$2s^22p^4(3P)3d$	$^4$ P	2.5	3	3.77071E+01	3.71888E+01
$2s^22p^4(3P)3d$	$^{4}P$	1.5	4	3.76644E+01	3.74741E+01
$2s^22p^4(3P)3d$	$^{4}P$	0.5	5	3.75753E+01	3.76035E+01
$2s^22p^4(3P)3d$	$^{2}F$	2.5*	4	3.70138E+01	3.74012E+01
$2s^22p^4(3P)3d$	$^{4}D$	1.5*	5	3.70854E+01	3.70494E+01
$2s^22p^4(3P)3d$	$^{4}D$	0.5*	6	3.72270E+01	3.71934E+01
$2s^22p^4(3P)3d$	$^{2}\mathbf{P}$	1.5*	6	3.68142E+01	3.67915E+01
$2s^22p^4(3P)3d$	$^{2}D$	2.5*	6	3.65054E+01	3.67031E+01
$2s^22p^4(1D)3d$	$^{2}S$	0.5	7	3.57421E+01	3.61810E+01
$2s^22p^4(1D)3d$	$^{2}P$	1.5	9	3.55234E+01	3.59614E+01
$2s^22p^4(1D)3d$	$^{2}P$	0.5	8	3.51764E+01	3.56351E+01
$2s^22p^4(1D)3d$	$^{2}D$	2.5	8	3.57401E+01	3.59395E+01
$2s^22p^4(1D)3d$	$^{2}D$	1.5	10	3.52638E+01	3.57080E+01
$2s^22p^4(1S)3d$	$^{2}D$	2.5	10	3.43638E+01	3.47949E+01
$2s^22p^4(1S)3d$	$^{2}D$	1.5	11	3.42001E+01	3.46318E+01
$2s^2p^5(3P^{\circ})3p$	$^{4}D$	2.5*	11	3.19894E+01	3.19627E+01
$2s^2p^5(3P^{\circ})3p$	$^{4}D$	1.5*	12	3.22407E+01	3.20794E+01
$2s^2p^5(3P^{\circ})3p$	$^{2}\mathbf{P}$	1.5	13	3.17478E+01	3.18661E+01
$2s^2p^5(3P^{\circ})3p$	$^{2}\mathbf{P}$	0.5	10	3.14956E+01	3.16811E+01
$2s^2p^5(3P^{\circ})3p$	$^4P$	2.5*	12	3.16228E+01	3.16811E+01
$2s^2p^5(3P^{\circ})3p$	$^{4}P$	1.5*	14	3.13684E+01	3.14825E+01
$2s^2p^5(3P^{\circ})3p$	$^{2}S$	0.5	13	3.05348E+01	3.08492E+01
$2s^2p^5(1P^{\circ})3p$	$^{2}D$	2.5	14	2.85413E+01	2.91679E+01
$2s^2p^5(1P^{\circ})3p$	$^{2}D$	1.5	17	2.87592E+01	2.93547E+01
$2s^2p^5(1P^{\circ})3p$	$^{2}\mathbf{P}$	1.5	18	2.83573E+01	2.90722E+01
$2s^2p^5(1P^{\circ})3p$	$^{2}\mathbf{P}$	0.5	14	2.84608E+01	2.91487E+01
$2s^22p^4(3P)5d$	$^{2}D$	2.5*	28	1.32603E+01	1.34385E+01
$2s^22p^4(3P)5d$	$^{2}F$	2.5*	36	1.25467E+01	1.25272E+01
$2s^22p^4(3P)5d$	$^{2}\mathbf{P}$	1.5*	43	1.23254E+01	1.22538E+01
$2s^22p^4(1D)5d$	$^{2}\mathbf{P}$	1.5	46	1.18837E+01	1.18893E+01
$2s^22p^4(1D)5d$	$^{2}\mathbf{P}$	0.5	36	1.18729E+01	1.18893E+01
$2s^22p^4(1D)5d$	$^{2}D$	1.5*	47	1.18561E+01	1.18893E+01
$2s^22p^4(1D)5d$	$^{2}F$	2.5*	40	1.18898E+01	1.18893E+01
$2s^22p^4(3P)6d$	$^{2}D$	2.5*	52	9.05237E+00	9.24666E+00
$2s^22p^4(1D)6d$	$^{2}\mathbf{P}$	0.5*	45	7.68379E+00	7.87976E+00
$2s^22p^4(1D)6d$	$^{2}D$	1.5*	64	7.63943E+00	7.87976E+00
1 \ /					

an equivalent electron state. The top line of each set provides the expected number of fine structure levels (Nlv) for the possible  $^{(2S+1)}L^{\pi}$  terms with the given configurations. In the set, the spin multiplicity (2S+1) and parity  $\pi$  are fixed, but L varies. Within parenthesis next to each L, all possible J-values associated with the LS term are specified. For example, last set of levels in Table 3a, the top line states that there are eight levels in total for terms  $^4L^{\circ}$  with L being S, P, and D: one of  $^4S_{3/2}^{\circ}$ , three of  $^4P_{5/2,3/2,1/2}^{\circ}$ , and four of  $^4D_{7/2,5/2,3/2,1/2}^{\circ}$ . This line is followed by set of the energy levels of same configurations. Nlv(c) at the end specifies total number of calculated J-levels found for the

**Table 3a.** Sample table of fine structure energy levels of Fe XVIII as sets of *LS* term components.  $C_t$  is the core configuration,  $\nu$  is the effective quantum number.

Eqv electron/unidentified levels, parity: o $2s^22p^5$											
$\begin{array}{cccccccccccccccccccccccccccccccccccc$			$J_t$	nl	2J	E (Ry)	ν	$SL\pi$			
$ \begin{array}{cccccccccccccccccccccccccccccccccccc$											
$\begin{array}{c ccccccccccccccccccccccccccccccccccc$	1										
Eqv electron/unidentified levels, parity: e $2s^22p^5$					1	-9.89033E+01		2 Po			
$ \begin{array}{cccccccccccccccccccccccccccccccccccc$											
$\begin{array}{c} \text{Nlv(c)} = 1\text{: set complete} \\ \hline \text{Nlv} = 3,  ^4L^e\text{: P (5 3 1 )/2} \\ 2s^22p^4  (3\text{Pe})  2  3s  5  -4.30800\text{E} + 01  2.74  4  \text{P e} \\ 2s^22p^4  (3\text{Pe})  0  3s  3  -4.28328\text{E} + 01  2.72  4  \text{P e} \\ 2s^22p^4  (3\text{Pe})  1  3s  1  -4.23643\text{E} + 01  2.74  4  \text{P e} \\ \hline \text{Nlv(c)} = 3\text{: set complete} \\ \hline \text{Nlv} = 2,  ^2L^e\text{: P (3 1 )/2} \\ 2s^22p^4  (3\text{Pe})  2  3s  3  -4.21900\text{E} + 01  2.77  2  \text{P e} \\ 2s^22p^4  (3\text{Pe})  0  3s  1  -4.19622\text{E} + 01  2.75  2  \text{P e} \\ \hline \text{Nlv(c)} = 2\text{: set complete} \\ \hline \text{Nlv} = 2,  ^2L^e\text{: D (5 3 )/2} \\ 2s^22p^4  (1\text{De})  2  3s  5  -4.14001\text{E} + 01  2.75  2  \text{D e} \\ 2s^22p^4  (1\text{De})  2  3s  3  -4.13657\text{E} + 01  2.75  2  \text{D e} \\ \hline \text{Nlv(c)} = 2\text{: set complete} \\ \hline \hline \text{Nlv} = 8,  ^4L^o\text{: S (3 )/2 P (5 3 1 )/2 D (7 5 3 1 )/2} \\ 2s^22p^4  (3\text{Pe})  1  3p  3  -4.08298\text{E} + 01  2.79  4  \text{SPD o} \\ 2s^22p^4  (3\text{Pe})  0  3p  5  -4.07880\text{E} + 01  2.79  4  \text{PD o} \\ 2s^22p^4  (3\text{Pe})  0  3p  5  -4.07880\text{E} + 01  2.79  4  \text{PD o} \\ 2s^22p^4  (3\text{Pe})  0  3p  1  -4.05343\text{E} + 01  2.80  4  \text{PD o} \\ 2s^22p^4  (3\text{Pe})  0  3p  1  -4.05343\text{E} + 01  2.80  4  \text{PD o} \\ \end{array}$											
$\begin{array}{c ccccccccccccccccccccccccccccccccccc$	*										
$\begin{array}{cccccccccccccccccccccccccccccccccccc$	Nlv(c) = 1	1: set co	mpl	ete							
$ \begin{array}{cccccccccccccccccccccccccccccccccccc$	Nlv = 3, 4	Le: P (	5 3	1)/2							
$ \begin{array}{cccccccccccccccccccccccccccccccccccc$	$2s^22p^4$	(3Pe)	2	3s	5	-4.30800E+01	2.74	4 Pe			
$\begin{array}{c} \text{Nlv(c)} = 3\text{: set complete} \\ \hline \text{Nlv} = 2,  ^2L^e\text{: P ( 3 1 )/2} \\ 2s^22p^4  \text{(3Pe)}  2  3s  3  -4.21900\text{E}+01  2.77  2  \text{P e} \\ 2s^22p^4  \text{(3Pe)}  0  3s  1  -4.19622\text{E}+01  2.75  2  \text{P e} \\ \hline \text{Nlv(c)} = 2\text{: set complete} \\ \hline \text{Nlv} = 2,  ^2L^e\text{: D ( 5 3 )/2} \\ 2s^22p^4  \text{(1De)}  2  3s  5  -4.14001\text{E}+01  2.75  2  \text{D e} \\ 2s^22p^4  \text{(1De)}  2  3s  3  -4.13657\text{E}+01  2.75  2  \text{D e} \\ \hline \text{Nlv(c)} = 2\text{: set complete} \\ \hline \hline \text{Nlv} = 8,  ^4L^o\text{: S ( 3 )/2 P ( 5 3 1 )/2 D ( 7 5 3 1 )/2} \\ 2s^22p^4  \text{(3Pe)}  1  3p  3  -4.08298\text{E}+01  2.79  4  \text{SPD o} \\ 2s^22p^4  \text{(3Pe)}  0  3p  5  -4.07880\text{E}+01  2.79  4  \text{PD o} \\ 2s^22p^4  \text{(3Pe)}  0  3p  1  -4.05343\text{E}+01  2.80  4  \text{PD o} \\ 2s^22p^4  \text{(3Pe)}  0  3p  1  -4.05343\text{E}+01  2.80  4  \text{PD o} \\ \hline \end{array}$	$2s^22p^4$	(3Pe)	0	3s	3	-4.28328E+01	2.72	4 Pe			
$\begin{array}{c ccccccccccccccccccccccccccccccccccc$	$2s^22p^4$	(3Pe)	1	3s	1	-4.23643E+01	2.74	4 Pe			
$ \begin{array}{cccccccccccccccccccccccccccccccccccc$	Nlv(c) = 3	3: set co	mpl	ete							
$ \begin{array}{cccccccccccccccccccccccccccccccccccc$	$Nlv = 2, ^{2}$	Le: P (	31)	)/2							
$ \begin{array}{cccccccccccccccccccccccccccccccccccc$	$2s^{2}2p^{4}$	(3Pe)	2	3s	3	-4.21900E+01	2.77	2 Pe			
$\begin{array}{c} \text{Nlv(c)} = 2\text{: set complete} \\ \hline \text{Nlv} = 2,  ^2L^e\text{: D ( 5 3 )/2} \\ 2s^22p^4  \text{(1De)}  2  3s  5  -4.14001\text{E}+01  2.75  2  \text{D e} \\ 2s^22p^4  \text{(1De)}  2  3s  3  -4.13657\text{E}+01  2.75  2  \text{D e} \\ \hline \text{Nlv(c)} = 2\text{: set complete} \\ \hline \text{Nlv} = 8,  ^4L^o\text{: S ( 3 )/2 P ( 5 3 1 )/2 D ( 7 5 3 1 )/2} \\ 2s^22p^4  \text{(3Pe)}  1  3p  3  -4.08298\text{E}+01  2.79  4  \text{SPD o} \\ 2s^22p^4  \text{(3Pe)}  0  3p  5  -4.07880\text{E}+01  2.79  4  \text{PD o} \\ 2s^22p^4  \text{(3Pe)}  0  3p  1  -4.05343\text{E}+01  2.80  4  \text{PD o} \\ \end{array}$			0	3s	1	-4.19622E+01	2.75	2 Pe			
$\begin{array}{cccccccccccccccccccccccccccccccccccc$		2: set co	mpl	ete							
$\begin{array}{cccccccccccccccccccccccccccccccccccc$	Nlv = 2. 2	Le: D (	53	)/2							
$ \begin{array}{cccccccccccccccccccccccccccccccccccc$					5	-4.14001E+01	2.75	2 De			
$\begin{aligned} &\text{Nlv(c)} = 2\text{: set complete} \\ &\text{Nlv} = 8, ^4L^o\text{: S ( 3 )/2 P ( 5 3 1 )/2 D ( 7 5 3 1 )/2} \\ &2s^22p^4 & \text{(3Pe)} & 1 & 3p & 3 & -4.08298E+01 & 2.79 & 4 \text{ SPD o} \\ &2s^22p^4 & \text{(3Pe)} & 0 & 3p & 5 & -4.07880E+01 & 2.79 & 4 \text{ PD o} \\ &2s^22p^4 & \text{(3Pe)} & 0 & 3p & 1 & -4.05343E+01 & 2.80 & 4 \text{ PD o} \end{aligned}$				3s				2 De			
NIv = 8, ${}^4L^o$ : S ( 3 )/2 P ( 5 3 1 )/2 D ( 7 5 3 1 )/2 2s <sup>2</sup> 2p <sup>4</sup> (3Pe) 1 3p 3 -4.08298E+01 2.79 4 SPD o 2s <sup>2</sup> 2p <sup>4</sup> (3Pe) 0 3p 5 -4.07880E+01 2.79 4 PD o 2s <sup>2</sup> 2p <sup>4</sup> (3Pe) 0 3p 1 -4.05343E+01 2.80 4 PD o		` /	mpl								
$\begin{array}{cccccccccccccccccccccccccccccccccccc$	*										
$2s^{2}2p^{4}$ (3Pe) 0 3p 5 -4.07880E+01 2.79 4 PD o $2s^{2}2p^{4}$ (3Pe) 0 3p 1 -4.05343E+01 2.80 4 PD o							2.79	4 SPD o			
$2s^22p^4$ (3Pe) 0 3p 1 $-4.05343E+01$ 2.80 4 PD o		` ′		_							
		` /									
20 2p (61 0) 2 6p / 110 17 7 21 61 21 66 1 2 6		` /									
$2s^22p^4$ (3Pe) 2 3p 5 -4.04793E+01 2.83 4 PD o		` /									
$2s^22p^4$ (3Pe) 1 3p 1 -4.00182E+01 2.82 4 PD o		` /									
$2s^22p^4$ (3Pe) 0 3p 3 -3.99897E+01 2.82 4 SPD o		` /									
$2s^22p^4$ (3Pe) 2 3p 3 -3.96485E+01 2.86 4 SPD o		` /									
Nlv(c) = 8: set complete	•	` ′			-	2.50.002.01	2.00	. 5120			
	(-/		r								

set. If NIv = NIv(c), the calculated energy set for the given terms is complete. The completeness of levels is checked by the program PRCBPID, which also detects the missing levels. A level may be mixed with more than one term. In case of multiple assignment of LS terms for a level, Hund's rule may be applied to determine the lower levels as explaind in Computation section. It may be noted that levels in the table are grouped consistently in energies and effective quantum numbers confirming the accuracy of identification.

#### 4.1.2. $J\pi$ format

In this format the fine structure levels are presented as sets, with descending energy order, of various  $J\pi$  symmetries. A sample is shown in Table 3b. The format is convenient for easy implementation in astrophysical models requiring large number of energy levels and corresponding transitions.

The top of the set specifies the total number of energy levels Nlv and the symmetry  $J\pi$ . Hence, following Table 3b, there are 74 fine structure levels of Fe XVIII with  $J\pi = (1/2)^e$ . The levels are identified by the configuration and LS term designation of the parent core, the outer electron quantum numbers (nl), absolute energy in Rydberg, the effective quantum number  $(\nu)$ , and the final LS term designation. A level may be assigned with one or more LS terms, as given in the last column, based on the same core term and configuration. However, for a mixed state, the dominant term designation may be determined from a

**Table 3b.** Sample table of fine structure energies in sets of various  $J\pi$  symmetries of Fe XVIII. Nlv is the total number of levels belonging to the specified symmetry.

			Level $E$ (Ry) $\nu$ $SL\pi$										
	Nlv = 74, $J$ pi = 1/2 e												
1	$2s^{2}2p^{5}$		1/2	-9.00804E+01		<sup>2</sup> Se							
2	$2s^22p^4(^3P_0^e)$	3s	1/2	-4.23643E+01	2.74	<sup>4</sup> Pe							
3	$2s^22p^4(^3P_0^e)$	3s	1/2	-4.19622E+01	2.75	<sup>2</sup> Pe							
4	$2s^22p^4(^1S_0^e)$	3s	1/2	-3.99696E+01	2.75	<sup>2</sup> Se							
5	$2s^22p^4(^3P_0^e)$	3d	1/2	-3.75753E+01	2.94	<sup>4</sup> PDe							
6	$2s^22p^4(^3P_0^e)$	3d	1/2	-3.72270E+01	2.95	<sup>4</sup> PDe							
7	$2s^22p^4(^3P_0^e)$	3d	1/2	-3.68446E+01	2.96	<sup>2</sup> Pe							
7	$2s^22p^4(^3P_0^{\tilde{e}})$	3d	1/2	-3.68446E+01	2.96	<sup>2</sup> Pe							
8	$2s^22p^4(^1D_0^e)$	3d	1/2	-3.57421E+01	2.95	<sup>2</sup> SPe							
9	$2s^22p^4(^1D_0^{e})$	3d	1/2	-3.51764E+01	2.97	<sup>2</sup> SPe							
10	$2s^2p^5(^3P_0^0)$	3p	1/2	-3.14956E+01	2.83	<sup>2</sup> SPe							
11	$2s^2p^5(^3P_0^{\circ})$	3p	1/2	-3.11994E+01	2.83	<sup>4</sup> PDe							
12	$2s^2p^5(^3P_0^0)$	3p	1/2	-3.10878E+01	2.84	<sup>4</sup> PDe							
13	$2s^2p^5(^3P_0^{\circ})$	3p	1/2	-3.05348E+01	2.88	<sup>2</sup> SPe							
14	$2s^2p^5(^1P_0^{\circ})$	3p	1/2	-2.84608E+01	2.85	<sup>2</sup> SPe							
15	$2s^2p^5(^1P_0^0)$	3p	1/2	-2.81570E+01	2.86	<sup>2</sup> SPe							
16	$2p^{6}(^{1}S_{0}^{e})$	3s	1/2	-2.24853E+01	2.78	<sup>2</sup> Se							
17	$2s^22p^4(^3P_0^e)$	4s	1/2	-2.18382E+01	3.78	<sup>4</sup> Pe							
18	$2s^22p^4(^3P_0^e)$	4s	1/2	-2.16367E+01	3.81	<sup>2</sup> Pe							
19	$2s^22p^4(^3P_0^{\tilde{e}})$	4d	1/2	-2.04748E+01	3.98	<sup>4</sup> PDe							
20	$2s^22p^4(^3P_0^{e})$	4d	1/2	-2.03390E+01	3.99	<sup>4</sup> PDe							
21	$2s^22p^4(^3P_0^e)$	4d	1/2	-1.97070E+01	3.97	<sup>2</sup> Pe							
22	$2s^22p^4(^1S_0^e)$	4s	1/2	-1.95086E+01	3.80	<sup>2</sup> Se							
23	$2s^22p^4(^1D_0^e)$	4d	1/2	-1.88196E+01	3.99	<sup>2</sup> SPe							
24	$2s^22p^4(^1D_0^e)$	4d	1/2	-1.86513E+01	4.01	<sup>2</sup> SPe							
25	$2s^22p^4(^3P_0^e)$	5s	1/2	-1.38412E+01	4.70	<sup>4</sup> Pe							
			••••	•••••									

variation of Hund's rule as a guideline, as mentioned before: the term with higher angular momentum lies lower in energy. Hund's rule may not necessarily apply to all cases, especially for low lying levels in complex ions. The order of calculated energy levels may not match exactly with that of the measured ones, and hence keeping all possible terms gives a guidance and establishes the completeness of fine structure components.

#### 4.2. Oscillator strengths for allowed E1 transitions

The allowed E1 ( $\Delta J = 0$ ,  $\pm 1$ ) transitions presented here are obtained from the BPRM method. The 1174 fine structure levels of Fe XVIII yield 141 869 ( $\approx 1.42 \times 10^5$ ) allowed E1 (dipole allowed and intercombination) transitions. The table of oscillator strengths of complete set of fine structure transitions is available electronically. It contains the level energies, oscillator strengths (f), line strengths (S) and the radiative decay rates (A). Although A, f, and S are related, all three are listed since different applications require one or the other quantity.

A sample set of transitions of Fe XVIII is presented in Table 4. The top of the table specifies the nuclear charge (Z=26) and number of electrons in the ion ( $N_{\rm elc}=9$ ). Then sets of oscillator strengths belonging to various pairs of symmetries  $J_i\pi_i-J_k\pi_k$  are given. The transition symmetries are expressed in the form of the statistical weight factors, g=2J+1, and parity  $\pi$  (=0 for even and =1 for odd parity) at the top of each set. For example, Table 4 presents transitions in levels of symmetries  $J=1/2^e-J=1/2^o$ . The next numbers are the number of bound levels belonging to each symmetry,  $N_{Ji}=74$  and  $N_{Jk}=73$  and the number of transitions,  $N_{Ji}\times N_{Jk}=5402$ ,

**Table 4.** Sample set of f-, S and A-values for allowed E1 transitions in Fe XVIII.

=	2.						
	26	9 .					
$I_i$		λ(Å)	$E_i$ (Ry)	$E_k$ (Ry)	f	S	$A_{ki}$ (s <sup>-1</sup> )
	2	0 2		5402			
1	1	103.94	-9.040E+01	-9.917E+01	4.623E-02	3.164E-02	2.855E+10
1	2	18.28	-9.040E+01	-4.053E+01	-7.548E-05	9.082E-06	1.508E+09
1	3	18.09	-9.040E+01	-4.002E+01	-4.260E-05	5.074E-06	8.685E+08
1	4	18.07	-9.040E+01	-3.997E+01	-1.636E-04	1.946E-05	3.341E+09
1	5	17.90	-9.040E+01	-3.949E+01	-6.923E-06	8.160E-07	1.442E+08
1	6	17.40	-9.040E+01	-3.803E+01	-3.143E-03	3.600E-04	6.922E+10
1	7	17.15	-9.040E+01	-3.727E+01	-1.191E-05	1.345E-06	2.699E+08
1	8	16.05	-9.040E+01	-3.361E+01	-1.154E-02	1.220E-03	2.991E+11
1	9	15.89	-9.040E+01	-3.305E+01	-5.631E-02	5.891E-03	1.488E+12
1	10	15.32	-9.040E+01	-3.093E+01	-9.511E-03	9.596E-04	2.702E+11
1	11	14.90	-9.040E+01	-2.924E+01	-1.293E-04	1.269E-05	3.885E+09
1	12	14.69	-9.040E+01	-2.835E+01	-7.287E-02	7.047E-03	2.254E+12
1	13	14.58	-9.040E+01	-2.789E+01	-3.955E-01	3.796E-02	1.241E+13
1	14	14.05	-9.040E+01	-2.554E+01	-5.587E-01	5.169E-02	1.889E+13
1	15	13.22	-9.040E+01	-2.145E+01	-4.162E-05	3.622E-06	1.589E+09
1	16	13.11	-9.040E+01	-2.091E+01	-1.076E-04	9.294E-06	4.175E+09
1	17	13.09	-9.040E+01	-2.080E+01	-1.018E-05	8.773E-07	3.960E+08
1	18	13.05	-9.040E+01	-2.057E+01	-1.961E-03	1.685E-04	7.683E+10
1	19	13.04	-9.040E+01	-2.052E+01	-4.347E-02	3.732E-03	1.705E+12
1	20	12.97	-9.040E+01	-2.011E+01	-4.034E-05	3.444E-06	1.601E+09
1	21	12.88	-9.040E+01	-1.967E+01	-6.203E-06	5.262E-07	2.493E+08
1	22	12.75	-9.040E+01	-1.895E+01	-1.177E-03	9.887E-05	4.827E+10
1	23	12.67	-9.040E+01	-1.849E+01	-8.563E-04	7.145E-05	3.557E+10
1	24	11.93	-9.040E+01	-1.399E+01	-1.519E-06	1.193E-07	7.124E+07
1	25	11.84	-9.040E+01	-1.342E+01	-9.775E-05	7.619E-06	4.653E+09

among them. The transitional parameters follow this line. The first two columns are level indices  $I_i$  and  $I_k$  whose identification can be found from the energy Table 3b, the third column is the transition wavelength ( $\lambda$ ) in Å. The wavelengths are obtained from  $E(\text{Å}) = 911.2671/E_{ik}$  (Ry), that is, no mass correction is considered. Hence, they are approximated wavelengths. (Readers may consult NIST website for the more accurate wavelengths). The fourth and fifth columns provide the energies  $E_i$ and  $E_k$  in Rydbergs of the transitional levels. The sixth column is f, the oscillator strength in length formulation. The sign of f indicates the upper and lower levels in transitions such that a negative value means that i is the lower level, while a positive value means k is the lower level. Column seven is line strength S, and the last column is transition probability or the radiative decay rate  $A_{ki}(s^{-1})$ . Spectroscopic notation of the transition can be obtained from Table 3b by referring to the values of  $J_i\pi_i$ ,  $I_i$ ,  $J_k\pi_k$ , and  $I_k$ . In the table the calculated energies have been replaced by the observed energies wherever available.

A subset of BPRM allowed transition probabilities for Fe XVIII has been reprocessed using observed energies to obtain the f- and A-values with spectroscopic notation. They are obtained from the calculated line strengths (S), the energy independent quantity. As the observed energies have lower uncertainties, use of the of the former improves the accuracy of the f- and A-values for the relevant transitions. This is a common procedure and is used in the NIST compilation. The astrophysical models also attempt to use observed transition energies to compute f- and A-values. This subset consists of 76 transitions of Fe XVIII (also available electronically). The reprocessed transitions are further ordered in terms of their configurations and LS terms. This enables one to obtain the f-values for LS multiplets and check the completeness of the set of fine structure components belonging to a given multiplet. However, the completeness depends also on the observed set of fine structure

**Table 5.** Sample table of dipole allowed and intercombination E1 transitions in Fe XVIII, grouped as fine structure components of LS multiplets. The calculated energies have been replaced by the observed energies.

$C_i - C_k$	$T_i - T_k$	$g_i$ :I- $g_j$ :K	$E_{ik}$	f	S	A
			(Å)			$(s^{-1})$
$2s^22p^5 - 2s^2p^6$	$^{2}P^{\circ} - ^{2}S^{e}$	2: 1- 2: 1	103.94	4.62E-02	3.16E-02	2.85E+10
$2s^22p^5 - 2s^2p^6$	$^2P^{\circ} - {}^2S^e$	4: 1- 2: 1	93.92	5.08E-02	6.28E-02	7.68E+10
LS	$^2P^{\circ} - {}^2S^e$	6- 2		4.93E-02	9.44E-02	1.05E+11
$2s^22p5 - 2s^22p^43P3s$	$^{2}P^{\circ} - {}^{4}P^{e}$	2: 1- 2: 2	16.11	5.54E-03	5.88E-04	1.42E+11
$2s^22p^5 - 2s^22p^43P3s$	$^{2}P^{\circ} - {}^{4}P^{e}$	4: 1- 2: 2	15.85	4.26E-04	8.88E-05	2.26E+10
$2s^22p^5 - 2s^22p^43P3s$	$^{2}P^{\circ} - {}^{4}P^{e}$	2: 1- 4: 1	16.09	4.71E-02	4.99E-03	6.06E+11
$2s^22p^5 - 2s^22p^43P3s$	$^{2}P^{\circ} - {}^{4}P^{e}$	4: 1- 4: 1	15.83	3.68E-02	7.67E-03	9.79E+11
$2s^22p^5 - 2s^22p^43P3s$	$^{2}P^{\circ} - {}^{4}P^{e}$	4: 1- 6: 1	16.07	4.31E-03	9.12E-04	7.42E+10
$2s^22p^5 - 2s^22p^43P3s$	$^{2}P^{\circ} - ^{2}P^{e}$	2: 1- 2: 3	16.03	7.47E-02	7.89E-03	1.94E+12
$2s^22p^5 - 2s^22p^43P3s$	$^{2}P^{\circ} - {}^{2}P^{e}$	4: 1- 2: 3	15.77	1.06E-02	2.20E-03	5.69E+11
$2s^22p^5 - 2s^22p^43P3s$	$^{2}P^{\circ} - {}^{2}P^{e}$	2: 1- 4: 2	16.27	1.90E-02	2.04E-03	2.40E+11
$2s^22p^5 - 2s^22p^43P3s$	$^2P^{\circ} - ^2P^{e}$	4: 1- 4: 2	16.00	2.52E-02	5.30E-03	6.55E+11
LS	$^{2}P^{\circ} - {^{2}P^{e}}$	6- 6		5.51E-02	1.74E-02	1.43E+12
$2s^22p^5 - 2s^22p^41S3s$	$^2P^{\circ} - {}^2S^e$	2: 1- 2: 4	15.45	2.00E-04	2.04E-05	5.60E+09
$2s^22p^5 - 2s^22p^41S3s$	$^{2}P^{\circ} - {^{2}S^{e}}$	4: 1- 2: 4	15.21	2.05E-02	4.12E-03	1.19E+12
LS	$^{2}P^{\circ} - {^{2}S^{e}}$	6- 2		1.37E-02	4.14E-03	1.18E+12
$2s^22p^5 - 2s^22p^43P3d$	$^{2}P^{\circ} - {}^{4}P^{e}$	2: 1- 2: 5	14.80	2.74E-05	2.67E-06	8.35E+08
$2s^22p^5 - 2s^22p^43P3d$	$^{2}P^{\circ} - {}^{4}P^{e}$	4: 1- 2: 5	14.58	8.02E-04	1.54E-04	5.03E+10
$2s^22p^5 - 2s^22p^43P3d$	$^{2}P^{\circ} - {}^{4}P^{e}$	2: 1- 4: 4	14.77	2.46E-03	2.40E-04	3.77E+10
$2s^22p^5 - 2s^22p^43P3d$	$^{2}P^{\circ} - {}^{4}P^{e}$	4: 1- 4: 4	14.55	2.10E-04	4.02E-05	6.61E+09
$2s^22p^5 - 2s^22p^43P3d$	$^{2}P^{\circ} - {}^{4}P^{e}$	4: 1- 6: 3	14.48	2.09E-06	3.99E-07	4.43E+07
$2s^22p^5 - 2s^22p^43P3d$	$^{2}P^{\circ} - ^{4}D^{e}$	2: 1- 2: 6	14.70	7.43E-02	7.19E-03	2.29E+12
$2s^22p^5 - 2s^22p^43P3d$	$^{2}P^{\circ} - {}^{4}D^{e}$	4: 1- 2: 6	14.49	4.53E-03	8.65E-04	2.88E+11
$2s^22p^5 - 2s^22p^43P3d$	$^{2}P^{\circ} - {}^{4}D^{e}$	2: 1- 4: 5	14.67	2.09E-01	2.02E-02	3.24E+12
$2s^22p^5 - 2s^22p^43P3d$	$^2P^{\circ} - {}^4D^e$	4: 1- 4: 5	14.45	1.50E-02	2.86E-03	4.80E+11
$2s^22p^5 - 2s^22p^41D3d$	${}^{2}P^{\circ} - {}^{2}S^{e}$	2: 1- 2: 7	14.47	8.40E-03	8.00E-04	2.68E+11
$2s^22p^5 - 2s^22p^41D3d$	$^{2}P^{\circ} - {^{2}S^{e}}$	4: 1- 2: 7	14.26	4.68E-04	8.79E-05	3.07E+10
LS	$^2P^{\circ} - {}^2S^e$	6- 2		3.11E-03	8.88E-04	2.98E+11
2 5 2 4						
$2s^22p^5 - 2s^22p^41D3d$	$^{2}P^{\circ} - {^{2}P^{e}}$	2: 1- 2: 8	14.34	2.93E-01	2.76E-02	9.49E+12
$2s^22p^5 - 2s^22p^41D3d$	$^{2}P^{\circ} - ^{2}P^{e}$	4: 1- 2: 8	14.14	1.18E-01	2.19E-02	7.86E+12
$2s^22p^5 - 2s^22p^41D3d$	$^{2}P^{\circ} - ^{2}P^{e}$	2: 1- 4: 9	14.42	2.79E-01	2.64E-02	4.47E+12
$2s^22p^5 - 2s^22p^41D3d$	$^{2}P^{\circ} - {^{2}P^{e}}$	4: 1- 4: 9	14.21	4.96E-01	9.29E-02	1.64E+13
LS	$^{2}P^{\circ} - {}^{2}P^{e}$	6- 6		6.00E-01	1.69E-01	1.97E+13

levels since the transitions correspond only to the observed levels. The *LS* multiplets are useful for various comparisons with other calculations and experiments where fine structure transitions can not be resolved. A partial set of these transitions is presented in Table 5. The level indices, I and K next to the statistical weight factors, are the calculated energy positions of the transitional symmetries. The table should be useful for comparison with experimental measurement, observation or spectral diagnostics.

The BPRM A-values for fine structure transitions in Fe XVIII are compared with those from other calculations in Table 6 (adopted from the compiled table at NIST database). There are 21 A-values of Fe XVIII listed in the table obtained by Cheng et al. (1979) and Fawcett (1984). Cheng et al. employed Dirac-Fock approximation which included Breit interaction and Lamb shift. Fawcett employed configuration interaction Hartree-Fock relativistic approximation in semi-empirical Cowan's code. In a recent work Witthoeft et al. (2006) present oscillator strengths from atomic structure calculations for a limited number of transitions for their work on collision strengths. Results from all three atomic structure calculations agree with each other for a number of transitions. NIST compilation of the atomic structure results also

**Table 6.** Comparison of present radiative decay rates, A-values, (in units of  $s^{-1}$ ) for Fe XVIII with those from previous calculations. The letter in the second column gives NIST accuracy rating.

λ	A:Ac	A	$C_i - C_j$	$SL\pi_i - SL\pi_j$	$g_i - g_j$			
Å	Others	Present						
			E1					
93.926	9.13e+10 <sup>a</sup> :C+	7.68e+10	$2s^22p^5 - 2s^2p^6$	$^{2}P^{\circ} - ^{2}S$	4 - 2			
103.939	$3.31e+10^a:C+$	2.85e+10	$2s^22p^5 - 2s^2p^6$	$^{2}P^{\circ} - {}^{2}S$	2 - 2			
15.766	$1.4e+12^{a,b}$ :D	5.69e+11	$2s^22p^5 - 2s^22p^4$ <sup>3</sup> P3s	$^{2}P^{\circ} - ^{2}P$	4 - 2			
16.026	$1.5e+12^{a,b}:D$	1.94e+12	$2s^22p^5 - 2s^22p^4$ <sup>3</sup> P3s	$^{2}P^{\circ} - {}^{2}P$	2 - 2			
15.847	2.0e+11 <sup>a</sup> :E	2.26e+10	$2s^22p^5 - 2s^22p^4$ <sup>3</sup> P3s	$^{2}P^{\circ} - {}^{4}P$	4 - 2			
16.072	$9.1e+10^{a}$ :E	7.42e+10	$2s^22p^5 - 2s^22p^4$ <sup>3</sup> P3s	$^{2}P^{\circ} - {}^{4}P$	4 - 6			
15.625	$1.1e+12^{a,b}:D$	1.02e+12	$2s^22p^5 - 2s^22p^4$ D3s	$^{2}P^{\circ} - ^{2}D$	4 - 6			
15.870	1.3e+12:D <sup>a,b</sup>	3.81e+11	$2s^22p^5 - 2s^22p^4$ D3s	$^{2}P^{\circ} - ^{2}D$	2 - 4			
14.152	$4.3e+12^{a,b}$ :E	2.44e+12	$2s^22p^5 - 2s^22p^4$ D3d	$^{2}P^{\circ} - ^{2}D$	4 - 4			
14.361	1.5e+13 <sup>a,b</sup> :E	1.44e+13	$2s^22p^5 - 2s^22p^4$ D3d	$^{2}P^{\circ} - ^{2}D$	2 - 4			
14.203	1.9e+13 <sup>a,b</sup> :E	1.64e+13	$2s^22p^5 - 2s^22p^4$ D3d	$^{2}P^{\circ} - ^{2}P$	4 - 4			
14.418	$3.2e+12^{a,b}$ :E	4.47e+12	$2s^22p^5 - 2s^22p^4$ D3d	$^{2}P^{\circ} - {}^{2}P$	2 - 4			
14.256	$1.6e+13^{a,b}:D$	3.07e+10	$2s^22p^5 - 2s^22p^4$ D3d	$^{2}P^{\circ} - {}^{2}S$	4 - 2			
14.469	$2.7e+12^{a,b}$ :D	2.68e+11	$2s^22p^5 - 2s^22p^4$ D3d	$^{2}P^{\circ} - {}^{2}S$	2 - 2			
15.209	$2.8e+11^{b}$ :E	1.19e+12	$2s^22p^5 - 2s^22p^4$ <sup>1</sup> S3s	$^{2}P^{\circ} - ^{2}S$	4 - 2			
13.919	$9.6e+10^{b}$ :E	6.94e+12	$2s^22p^5 - 2s^22p^4$ S3d	$^{2}P^{\circ} - ^{2}D$	4 - 4			
13.954	$1.1e+12^{a,b}$ :D	1.0e + 12	$2s^22p^5 - 2s^22p^4$ <sup>1</sup> S3d	$^{2}P^{\circ} - ^{2}D$	4 - 6			
14.121	$1.5e+13^{a,b}$ :D	6.68e+12	$2s^22p^5 - 2s^22p^4$ <sup>1</sup> S3d	$^{2}P^{\circ} - ^{2}D$	2 - 4			
E2,M1								
974.86	1.9e+00 <sup>a,b</sup> :D	1.98	$2s^22p^5 - 2s^22p^5 : E2$	$^{2}P^{\circ} - ^{2}P^{\circ}$	4 - 2			
974.86	1.93e+04a:C	1.94e+04	$2s^22p^5 - 2s^22p5 : M1$	$^2P^{\circ} - ^2P^{\circ}$	4 - 2			
		Lif	Tetime $(10^{-12} s)$					
λ	Expt	Present	$C_i - C_i$	$SL\pi_i - SL\pi_i$	$g_i - g_j$			
93.9	$12.2 \pm 0.8^{c}$	13.02	$2s^22p^5 - 2s^2p^6$	$^{2}P^{\circ} - ^{2}S$	4 - 2			

<sup>&</sup>lt;sup>a</sup> Cheng et al. (1979), <sup>b</sup> Fawcett (1984), <sup>c</sup> Buchet et al. (1980).

assigns its evaluated accuracy estimation (Ac) for the A-values and are denoted by the alphabetic notation next to them. Varying degrees of agreement can be seen between the present BPRM radiative decay rates and the earlier ones. The agreement is good for transitions, such as,  $2s^22p^5(^2P^\circ)-2s2p^6(^2S), 2s^22p^5(^2P^\circ)-2s^22p^4\ ^1D3d(^2P).$  However, it is poor for component transitions, such as, for  $2s^22p^5(^2P^\circ_{3/2})-2s^22p^4\ ^3P3s(^4P_{1/2}), 2s^22p^5(^2P^\circ_{3/2})-2s^22p^4\ ^1D3d(^2S_{1/2}).$ 

It appears that the wavefunctions of some transitional levels are sensitive to some transitions obtained in the Breit-Pauli R-matrix and atomic structure approaches. Present atomic structure calculations for the forbidden transitions also generated E1 transitions. Some of those transitions agree better with the earlier atomic structure results and some show differences. These transitions are not presented as it is a smaller set and includes less number of configurations than the BRRM calculations.

One main reason for the differences in the present BRPM and earlier atomic structure results is from the two different approaches that include different contributions of correlation configurations. The BPRM method does not allow semi-empirical adjustments that can be used in atomic structure calculations. The coupling coefficients from many channels for each symmetry are computed internally. The BPRM calculations include effects of more correlation configurations than the earlier ones and hence are be expected to be more accurate. However, a possible reason for difference is in the discrepancy of exact spectroscopic identification of levels. The other difference can come from the effects of Breit interaction for very weak transitions. The BRRM method does not include the contribution of the two-body Breit interaction. Hence for those weak transitions where relativistic effects are important, Breit interaction can play a significant role. The A-values for such transitions are to used with caution. Comparison with experimental measurements can provide a much better judgement on accuracy of the theoretical

**Table 7.** Sample set of fine strucuture levels of Fe XVIII and their relative energies for which forbidden transitions have been obtained. The configuration indices (Cf) correspond to  $2s^22p^5(1)$ ,  $2s2p^6(2)$ ,  $2s^22p^43s(3)$ ,  $2s^22p^43p(4)$ ,  $2s^22p^43d(5)$ ,  $2s^22p^44s(6)$ ,  $2s^22p^44p(7)$ ,  $2s^22p^44d(8)$ ,  $2s^22p^44f(9)$ ,  $2s2p^53s(10)$ ,  $2s2p^53p(11)$ ,  $2s2p^53d(12)$ ,  $2s2p^54s(13)$ ,  $2s2p^54p(14)$ ,  $2s2p^54d(15)$ .

ie	SLp (cf)	2J	E (Ry)
1	2Po(1)	3	0.00000E+00
2	2Po(1)	1	9.34770E-01
3	2Se(2)	1	9.70230E+00
4	4Pe(3)	5	5.66990E+01
5	2Pe(3)	3	5.69370E+01
6	4Pe(3)	1	5.75030E+01
7	4Pe(3)	3	5.75730E+01
8	2Pe(3)	1	5.77980E+01
9	2De(3)	5	5.83210E+01
10	2De(3)	3	5.83560E+01
11	4Po(4)	3	5.89657E+01
12	4Po(4)	5	5.90004E+01
13	4Po(4)	1	5.92534E+01
14	4Do(4)	7	5.93035E+01
15	2Do(4)	5	5.93169E+01
16	2Po(4)	1	5.97736E+01
17	4Do(4)	3	5.97958E+01
18	4Do(4)	1	5.98248E+01
19	2Do(4)	3	5.99582E+01
20	2Se(3)	1	5.99170E+01
21	4Do(4)	5	6.00805E+01
22	4So(4)	3	6.01290E+01
23	2So(4)	1	6.02730E+01
24	2Po(4)	3	6.03208E+01
25	2Fo(4)	5	6.06436E+01

numbers. Using the beam-foil technique, Buchet et al. (1980) measured the lifetime of level  $2s2p^6$  <sup>2</sup>S to be  $12.2 \pm 0.8$  ps. The present lifetime for this level is 13.02 ps agreeing with the upper limit of the experiment while Cheng et al. give a much lower lifetime of 8.1 ps.

#### 4.3. Radiative decay rates for the forbidden transitions

The forbidden transitions are relatively weak and are observed mainly in the low-lying levels. However, they provide important diagnostics of the ambient conditions. The forbidden transitions of higher order electric (E2, E3) and magnetic (M1, M2) multipoles are presented for levels up to n=4, that is, up to 4f. They are obtained from atomic structure calculations using SUPERSTRUCTURE. A total of 29 682 such transitions obtained for 243 fine structure levels of fifteen configurations as listed in Table 7. The table presents a subset of the complete set of energy levels for forbidden transitions in ascending order. Comparison of these levels with the measured values (NIST compilation) shows agreement within 1% for most levels. The largest difference is 3.4% for the level  $2s2p^5(^1P^\circ)3p^2D$ . The forbidden transitions are reprocessed with the available observed energies for improved accuracy.

Sample subsets of the complete set of radiative decay rates for the forbidden transitions in Fe XVIII are given in Table 8. The parity remains unchanged for the E2 and M1 transitions and hence are presented together. On the otherhand, parity changes for E3 and M2 transitions which are presented together in Table 8. The complete sets of energies and the transitions are processed from SUPERSTRUCTURE output to standard spectroscopic notation and are available electronically.

Present *A*-coefficients for forbidden transitions are compared with previous works in Table 6. The only two transitions within

AM1

**Table 8.** Sample table of radiative decay rates in  $s^{-1}$  for the forbidden electric quadrupole (AE2), electric octupole (AE3), magnetic dipole (AM1) and magnetic quadrupole (AM3) transitions in Fe XVIII. The level numbers (i, j) and configurations indices  $(C_i, C_j)$  correspond to those in Table 7, that is,  $2s^22p^5(1)$ ,  $2s2p^6(2)$ ,  $2s^22p^43s(3)$ ,  $2s^22p^43p(4)$ ,  $2s^22p^43d(5)$ ,  $2s^22p^44s(6)$ ,  $2s^22p^44p(7)$ ,  $2s^22p^44d(8)$ ,  $2s^22p^44f(9)$ ,  $2s2p^53s(10)$ ,  $2s2p^53p(11)$ ,  $2s2p^53d(12)$ ,  $2s2p^54s(13)$ ,  $2s2p^54p(14)$ ,  $2s2p^54d(15)$ . T denotes the LS term,  $SL\pi$ , and  $N_{tr}$  is the number of transitions.

 $E_j$  (Ry)

 $T_i C_i - T_j C_j$   $g_i - g_j$   $\lambda$  (Å)  $E_i$  (Ry)

i - j	$T_i C_i - T_j C_j$	$g_i - g_j$		$E_i$ (Ky)	$E_j$ (Ky)	AEZ	AIVII
		E		$N_{\rm tr} = 2152$	22		
1 - 2	2Po 1 – 2Po 1	4 - 2	974.86	0.00E+00	9.35E-01	1.98E+00	1.94E+04
3 - 4	2Se 2 - 4Pe 3	2 - 6	19.39	9.70E+00	5.67E+01	3.40E+05	0.00E+00
3 - 5	2Se 2 - 2Pe 3	2 - 4	19.29	9.70E+00	5.69E+01	4.43E+05	2.00E+02
4 - 5	4Pe 3-2Pe 3	6 - 4	3828	5.67E+01	5.69E+01	2.51E-04	1.73E+02
3 - 6	2Se 2-4Pe 3	2 - 2	19.06	9.70E+00	5.75E+01	0.00E+00	3.97E+02
4 - 6	4Pe 3 – 4Pe 3	6 - 2	1133	5.67E+01	5.75E+01	6.05E-01	0.00E+00
5 - 6	2Pe 3 – 4Pe 3	4 - 2	1610	5.69E+01	5.75E+01	1.27E-02	2.80E+03
3 - 7	2Se 2-4Pe 3	2 - 4	19.04	9.70E+00	5.76E+01	6.57E+04	4.88E+02
4 - 7	4Pe 3 – 4Pe 3	6 - 4	1042	5.67E+01	5.76E+01	3.47E-01	1.19E+04
5 – 7	2Pe 3 – 4Pe 3	4 - 4	1432	5.69E+01	5.76E+01	3.45E-02	1.53E+03
6 - 7	4Pe 3 – 4Pe 3	2 - 4		5.75E+01	5.76E+01	4.00E-08	6.30E+00
3 - 8	2Se 2 – 2Pe 3	2 - 2		9.70E+00	5.78E+01	0.00E+00	4.44E+02
4 - 8	4Pe 3 – 2Pe 3	6 - 2		5.67E+01	5.78E+01	2.16E-02	0.00E+00
5 - 8	2Pe 3 – 2Pe 3	4 - 2		5.69E+01	5.78E+01	3.90E-01	1.11E+04
6 - 8	4Pe 3 – 2Pe 3	2 - 2		5.75E+01	5.78E+01	0.00E+00	2.13E+01
7 - 8	4Pe 3 – 2Pe 3	4 - 2		5.76E+01	5.78E+01	2.91E-04	3.41E+01
3 - 9	2Se 2 – 2De 3	2 - 6		9.70E+00	5.83E+01	4.23E+06	
4 - 9	4Pe 3 – 2De 3	6 – 6		5.67E+01	5.83E+01	3.40E+00	1.60E+04
5 – 9	2Pe 3 – 2De 3	4 – 6		5.69E+01	5.83E+01	2.03E-01	4.85E+02
6-9	4Pe 3 – 2De 3	2 – 6		5.75E+01	5.83E+01	7.68E-03	0.00E+00
7 – 9	4Pe 3 – 2De 3	4 – 6		5.76E+01	5.83E+01	1.28E-02	1.02E+03
8 - 9	2Pe 3 – 2De 3	2 - 6		5.78E+01	5.83E+01	1.09E-03	0.00E+00
3 – 10	2Se 2 – 2De 3	2 - 4		9.70E+00	5.84E+01	4.49E+06	2.57E+00
4 - 10	4Pe 3 – 2De 3	6 - 4		5.67E+01	5.84E+01	1.36E+00	2.59E+03
5 – 10	2Pe 3 – 2De 3	4 – 4		5.69E+01	5.84E+01	2.25E+00	1.31E+04
6 – 10	4Pe 3 – 2De 3	2 - 4		5.75E+01	5.84E+01	4.39E-02	9.07E+01
7 – 10	4Pe 3 – 2De 3	4 - 4		5.76E+01	5.84E+01	5.62E-02	8.49E+01
		Е		$2, N_{\rm tr} = 816$	0		
i - j	$T_i C_i - T_j C_j$	$g_i - g_j$		$E_i$ (Ry)	$E_j$ (Ry)	AE3	AM2
2-4	2Po 1 – 4Pe 3	2-6		9.35E-01	5.67E+01	1.57E+04	2.54E+04
2 - 9	2Po 1 – 2De 3	2 - 6		9.35E-01	5.83E+01	2.59E+05	2.66E+05
3 – 12	2Se 2 – 4Po 4	2 – 6		9.70E+00	5.90E+01	7.74E+00	1.64E+01
6 – 12	4Pe 3 – 4Po 4	2 – 6		5.75E+01	5.90E+01	7.39E-06	5.18E-02
8 – 12	2Pe 3 – 4Po 4	2 – 6		5.78E+01	5.90E+01	5.23E-07	2.09E-02
4 - 13	4Pe 3 – 4Po 4	6 - 2		5.67E+01	5.93E+01	7.48E-04	7.62E-02
9 – 13	2De 3-4Po 4	6 – 2		5.83E+01	5.93E+01	2.28E-06	9.51E-03
3 – 14	2Se 2 – 4Do 4	2 - 8		9.70E+00	5.93E+01	4.31E+01	0.00E+00
5 – 14	2Pe 3 – 4Do 4	4 - 8		5.69E+01	5.93E+01	1.67E-03	2.13E-01
6 – 14	4Pe 3 – 4Do 4	2 - 8		5.75E+01	5.93E+01	4.21E-04	0.00E+00
7 – 14	4Pe 3 – 4Do 4	4 - 8		5.76E+01	5.93E+01	2.63E-04	2.67E-01
8 – 14	2Pe 3 – 4Do 4	2 - 8		5.78E+01	5.93E+01	2.82E-06	0.00E+00
10 – 14	2De 3 – 4Do 4	4 - 8		5.84E+01	5.93E+01	1.42E-07	7.00E-03
3 – 15	2Se 2 – 2Do 4	2 – 6		9.70E+00	5.93E+01	5.00E+01	7.81E+02
6 – 15	4Pe 3 – 2Do 4	2 – 6		5.75E+01	5.93E+01	3.11E-05	2.75E-02
8 – 15	2Pe 3 – 2Do 4	2 - 6		5.78E+01	5.93E+01	1.33E-04	1.69E-02
4 – 16	4Pe 3 – 2Po 4	6 - 2		5.67E+01	5.98E+01	7.63E-03	7.21E-01
9 – 16	2De 3 – 2Po 4	6 - 2		5.83E+01	5.98E+01	6.55E-05	2.39E-02
4 – 18	4Pe 3 – 4Do 4	6 - 2		5.67E+01	5.98E+01	3.95E-02	4.60E-04
9 – 18	2De 3 – 4Do 4	6 - 2		5.83E+01	5.98E+01	5.20E-06	3.80E-03
12 – 20	4Po 4 – 2Se 3	6-2		5.90E+01	5.99E+01	1.68E-07	4.80E-03
14 - 20	4Do 4 – 2Se 3	8 - 2		5.93E+01	5.99E+01	9.01E-08	0.00E+00
15 - 20	2Do 4 – 2Se 3	6 - 2		5.93E+01	5.99E+01	6.25E-08	1.65E-04
3 - 21	2Se 2 – 4Do 4	2 - 6	18.09		6.01E+01	2.76E+00	3.84E+02
6 - 21	4Pe 3 – 4Do 4	2 - 6		5.75E+01	6.01E+01	5.56E-04	2.66E-02
8 - 21	2Pe 3 – 4Do 4	2 - 6		5.78E+01	6.01E+01	1.27E-03	2.51E-02
3 - 21 20 - 21	2Se 3 – 4Do 4	2 - 6		5.78E+01 5.99E+01	6.01E+01	7.40E-14	1.60E-08
4 - 23	4Pe 3 – 2So 4	6 - 2		5.67E+01	6.03E+01	3.24E-02	2.41E+01
	.20 3 - 200 4	0 .2	254.71	5.07E 101		J.27L-02	
9 - 23	2De 3 - 2So 4	6 - 2	466 83	5 83F±01	6.03F + 01	1.07F-04	6.35F-03
9 – 23	2De 3 – 2So 4	6 - 2		5.83E+01	6.03E+01	1.07E-04	6.35E-03

the ground state term,  $2s^22p^5(^2P_{3/2}^\circ) - 2s^22p^5(^2P_{1/2}^\circ)$ , of types E2 and M1 are available in the NIST compilation. The E2 transition corresponds to the important EUV line prominently observed, for example, in the solar corona. Present rates for both the E2 and M1 transitions agree almost exactly with those by

Cheng et al. (1979) and Fawcett (1984). This reconfirms the accuracy of the earlier value.

#### 5. Conclusion

Results from large scale relativistic Breit-Pauli calculations for fine structure levels and allowed and forbidden transitions for Fe XVIII are presented. Very good agreement (most of them are within 1%) is found for the energies with those of the measured levels.

The dipole allowed and intercombination electric E1 transitions are obtained from ab initio relativistic Breit Pauli R-matrix (BPRM) method in the close coupling approximation and represent about 142 000 transitions. Although these transitions show varying degree of agreement with the earlier relativistic atomic structure calculations by Cheng et al. (1979) and Fawcett (1984), present lifetime agrees much better with the single measurement available. The weak transitions should be treated with caution since relativistic two body corrections, which may be important for these transitions, are not considered. However, the present oscillator strengths and radiative decay rates should provide overall good data for astrophysical plasma modeling. The forbidden transitions are obtained from configuration interaction atomic structure calculations using SUPERSTRUCTURE and show very good agreement with the two transitions available from the NIST database. The present A-values are expected to be accurate enough for most diagnostic applications.

The present results for fine structure levels and transitions exceed by far those currently available. The results from the present work should be useful in the analysis of X-ray, Extreme Ultraviolet, Ultraviolet, and optical spectra from astrophysical and laboratory sources where non-local thermodynamic equilibrium (NLTE) atomic models with many excited levels are needed.

All data are available electronically at CDS and from the author at nahar@astronomy.ohio-state.edu

Acknowledgements. This work was partially supported by NASA (05-APR05-4 and APRA-2006) program. The computational work was carried out on the Cray SV1 at the Ohio Supercomputer Center in Columbus, Ohio.

#### References

Berrington, K. A., Burke, P. G., Butler, K., et al. 1987, J. Phys. B, 20, 6379 Berrington, K. A., Eissner, W. B., & Norrington, P. H. 1995, Comput. Phys. Commun., 92, 290

Buchet, J. P., Buchet-Poulizac, M. C., Denis, A., Desesquelles, A., & Druetta, M. 1980, Phys. Rev. A, 22, 2061

Cheng, K. T., Kim, Y.-K., & Desclaux, J. P. 1979, At. Data Nucl. Data Tables, 24, 111

Eissner, W. 1991, in The Effects of Relativity on Atoms, Molecules, and the Solid State, ed. S. Wilson, et al. (New York: Plenum Press), 55

Eissner, W., & Zeippen, C. J. 1981, J. Phys. B, 14, 2125

Eissner, W., Jones, M., & Nussbaumer, H. 1974, Comput. Phys. Commun, 8, 270 Fawcett, B. C. 1984, At. Data Nucl. Data Tables, 31, 495

Hummer, D. G., Berrington, K. A., Eissner, W., et al. 1993, A&A, 279, 298 (IP)

Nahar, S. N. 2000, A&AS, 127, 253

Nahar, S. N. 2003, A&A, 413, 779

Nahar, S. N., & Pradhan, A. K. 1999, A&AS, 135, 347

Nahar, S. N., & Pradhan, A. K. 2000, Phys. Scr., 61, 675

Nahar, S. N., Delahaye, F., Pradhan, A. K., & Zeippen, C. J. 2000, A&AS, 144, 141

Nahar, S. N., Eissner, W., Chen, G. X., & Pradhan, A. K. 2003, A&A, 408, 789 NIST compilation for the energy levels and lines is available from the website, http://physics.nist.gov/cgi-bin/AtData/main\_asd

Scott, N. S., & Burke, P. G. 1980, J. Phys. B, 12, 4299

Scott, N. S., & Taylor, K. T. 1982, Comput. Phys. Commun., 25, 347

Witthoeft, M. C., Badnell, N. R., Zanna, G. Del, Berrington, K. A., & Pelan, C. 2006, A&A, 446, 361